PAPER

CrossMark
← click for updates

Highly improved performance of Zn^II tetraarylporphyrinates in DSSCs by the presence of octyloxy chains in the aryl rings†

A. Orbelli Biroli,*[a] F. Tessore,[b] V. Vece,[b] G. Di Carlo,[b] P. R. Mussini,[b] V. Trifiletti,[c] L. De Marco,[c] R. Giannuzzi,[c] M. Manca[c] and M. Pizzotti[b]

Three new β-substituted Zn^II-tetraarylporphyrinate dyes (**1–3**), bearing octyloxy chains at the *o,o*-, *o,p*- or *o*-positions of the four phenyl groups respectively, were synthesized, characterized and investigated as sensitizers for DSSCs. In particular, the alkoxy group position strongly influences their electronic absorption and electrochemical features. Improvements in power conversion efficiency ranging from 40% to 80% were obtained with respect to a reference dye (**4**) characterized by the presence of sterically bulky *t*-butyl groups at the *m*-positions.

Introduction

In the field of dye-sensitized solar cells (DSSCs),[1] Ru^II-poly-piridyl-based complexes reach efficiency values (η) of over 11%,[2–4] whereas metal-free organic dyes reach efficiencies around 10% at best.[1,5]

A comparable performance of Ru^II sensitizers has been attained by a push–pull Zn^II diarylporphyrinate with a diarylamino donor group directly linked to the *meso*-position of the porphyrinic ring (YD2).[6]

Because of the chemical, photochemical and thermal stability of metal porphyrinates, a large amount of work has been devoted to develop new porphyrinic dye structures for DSSC devices. Two strong absorption bands in the visible region also give them excellent light-harvesting efficiency; moreover, it is possible to fine tune their photophysical properties through a variety of substituents, which can be linked at the *meso* and/or β-pyrrolic position of the porphyrinic ring.[5]

However, lower efficiencies for porphyrinic dyes have been observed in the past, compared to N719, a widely used standard Ru^II dye. In fact, they suffer from aggregation by π–π stacking interactions,[5] which reduces the efficiency of electron injection, and show low V_{OC} values. Such low values are generally attributed to charge recombination between the electron injected

from the dye into TiO$_2$ and I$_3^-$ species of the redox shutter,[1,7] but it may also depend on the shorter electron lifetime.[8] Mozer *et al.* have supported this evidence suggesting an interaction between the positively charged metal centre and the I$_3^-$ of the electrolyte, which may promote a faster recombination reaction with the injected electron due to its closer proximity to the TiO$_2$ photoanode surface.[8,9]

A rational-design strategy has been proposed by introducing long alkoxy chains at the *ortho*-positions of the two opposite phenyl rings into the structure of *meso*-disubstituted push–pull Zn^II diarylporphyrinates, in order to envelop the porphyrinic ring,[10] thus, reducing π–π aggregation and hindering a facile interaction between the Zn^II centre and I$_3^-$.[11]

Hupp and co-workers first presented this strategy,[12,13] achieving an efficiency of η = 5.5%, with the ZnPDCA dye, which was found to be comparable with that measured for N719 under the same conditions.[13] Lin, Diau *et al.* confirmed the effectiveness of this approach when extended to *meso* push–pull Zn^II diarylporphyrinates, obtaining an efficiency improvement of 9% in the case of two phenyl rings bearing dodecoxyl chains (–OC$_{12}$H$_{25}$) at the *ortho*-positions (LD14, η = 10.17%) instead of bulky *t*-butyl groups at the *meta*-positions (LD13, η = 9.34%).[11]

The same strategy applied to YD2, with the addition of octyloxy (–OC$_8$H$_{17}$) chains, attained a higher performance (η over 12%), but only when the DSSC was co-sensitized with an organic dye and a Co-based redox electrolyte was used.[14]

Despite the interesting light-conversion efficiencies, which were very recently displayed by this series of *meso* push–pull Zn^II diarylporphyrinates, with or without co-sensitizer,[15–17] a multi-step synthesis is required reducing overall yields;[6,10–12,14,18] this also applies to basic porphyrinic ring synthesis.[19–22]

On the contrary, tetraarylporphyrins are easily achievable by the direct condensation of pyrrole and an aryl aldehyde.[21,22]

[a]Istituto di Scienze e Tecnologie Molecolari del CNR (CNR-ISTM), Via C. Golgi 19, 20133 Milano, Italy. E-mail: a.orbelli@istm.cnr.it

[b]Dipartimento di Chimica, Università degli Studi di Milano, Unità di Ricerca dell'INSTM, Via C. Golgi 19, 20133 Milano, Italy

[c]Center for Biomolecular Nanotechnologies (CBN), Fondazione Istituto Italiano di Tecnologia (IIT), Via Barsanti 1, 73010 Arnesano, Italy

Moreover, they can be functionalized in β-pyrrolic position by relatively few synthetic steps,[23,24] and these porphyrinic dyes may present light-conversion efficiencies of up to 7.1%.[25]

Recently, some of us reported a straightforward synthetic route, based on microwave-enhanced Sonogashira coupling,[26] which improves the overall yields of Zn[II]-tetraarylporphyrinate dyes monosubstituted in β-pyrrolic position.[27] Under the same DSSC fabrication conditions, these porphyrinic dyes have shown comparable or better light-conversion efficiencies with respect to those of some correlated *meso*-disubstituted push–pull Zn[II] diarylporphyrinates.[27]

Here, we present the synthesis, characterization and photovoltaic performances in DSSCs of a series of three new Zn[II]-tetraarylporphyrinate dyes (**1–3**, see Fig. 1), bearing octyloxy ($-OC_8H_{17}$) chains at the *ortho,ortho*- (*o,o*-), *ortho,para*- (*o,p*-) or *ortho*- (*o*-) positions of the four phenyl groups, respectively.

Compound **4**, characterized by the presence of sterically bulky *t*-butyl groups in *meta* positions of the four phenyl rings, has been taken into account as a reference dye.[27]

Results and discussion

Synthesis

The porphyrinic cores of **1** and **3** have already been reported and investigated for other applications.[28] However, to the best of our knowledge, the β-substitution for these types of porphyrins has never been reported, nor has their use in DSSCs.

The synthesis of the basic porphyrinic ring of **1** has been previously proposed by Bhyrappa *et al.*[29] in three synthetic steps, with an assessable overall yield in the range of 7.5% to 8.8%, starting from the 5,10,15,20-tetrakis(2′,6′-dimethoxyphenyl) porphyrinic core, obtained from the condensation of 2,6-dimethoxybenzaldehyde with pyrrole.[29,30]

Herein, we obtained the porphyrinic core of **1** by direct condensation between 2,6-dioctyloxybenzaldehyde and pyrrole under Lindsey's acidic condition.[21]

However, first attempts were carried out using CF_3COOH or $BF_3 \cdot Et_2O$ as the catalyst, but we were only able to obtain a polymer species because the reaction ran too quickly. To slow down the reaction, we adopted a heterogeneous catalyst, such as $InCl_3$, which is known to be a mild Lewis acid for the large-scale synthesis of dipyrromethanes,[20] obtaining a 13% yield but with a catalytic amount of 50 mol%.

The best yields were reached using $In(OTf)_3$ as an acidic catalyst,[31] which promotes the cyclization reaction when added in a catalytic amount of 6 mol%, allowing to obtain the porphyrinic core of **1** in a single synthetic step with a 16% yield (see ESI†).

Porphyrinic cores of **2** and **3** were instead synthesized from 2,4-dioctyloxy- and 2-octyloxy-benzaldehyde, respectively, under Lindsey's standard conditions with CF_3COOH as a catalyst (see ESI†). In these cases the porphyrin cores are obtained as an atropisomeric mixture, due to the mono *ortho*-substitution of the *meso* phenyl groups, perpendicular to the porphyrinic ring. Because the single isomers, difficult to separate and identify, tend to be converted again in the atropisomeric mixture upon heating either as free porphyrins or as Zn[II] porphyrinates, we decided to proceed working directly on the atropisomeric mixture. The full synthetic steps are described in detail in ESI† and consist in the same synthetic routes already reported in the literature.[27]

Electronic absorption spectroscopy

In Fig. 2 the UV-vis absorption spectra of **1–4**, recorded in THF solution, are reported and the relative data are collected in Table 1.

All Zn[II] porphyrinates **1–3** show the typical absorption B and Q bands in the visible region of the spectrum and present a B band with a red-shifted shoulder at about 460 nm. This may be rationalized on the basis of some deviation from the "Gouterman four-orbital simple model" due to the presence of a strong electron-acceptor group on the substituent at β position, as previously suggested.[27,32,33] While **2** and **3** show spectra very similar to that of reference dye **4**. **1** presents a B band with a broadened shoulder and clearly red-shifted Q bands (see Table 1).
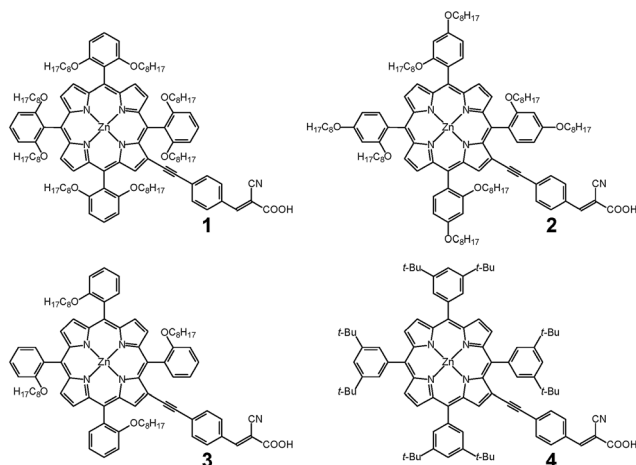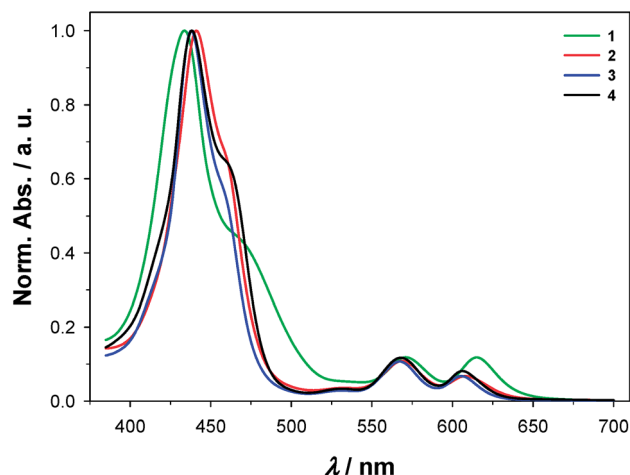

Fig. 1 Molecular structure of dyes **1–4**.

Fig. 2 UV-vis spectra of dyes **1–4** in THF solution.

This journal is © The Royal Society of Chemistry 2015

J. Mater. Chem. A, 2015, **3**, 2954–2959 | **2955**

Table 1 Spectrophotometric data for dyes **1–4** in THF solution

Dye	λ_B/nm (log ε)	λ_Q/nm (log ε)	
1	434 (4.87)	571 (3.95)	615 (3.95)
2	441 (5.29)	569 (4.32)	608 (4.11)
3	438 (5.29)	567 (4.32)	605 (4.11)
4	438 (5.30)	568 (4.36)	606 (4.20)

Unexpectedly, **1** shows the lowest coefficients of molar absorption. This characteristic has also been confirmed in a chlorinated solvent such as CH_2Cl_2 (see Fig. S2,† where electronic absorption spectra of **1** are compared to those of **3**).

Moreover, the shape and position of the absorption bands are influenced by the nature of solvents (see Fig. S2 and S3†), supporting our previous suggestion that, in Zn^{II}-tetraaryl-porphyrinates substituted at β-pyrrolic position both B and Q bands contribute to charge-transfer transitions.[27] However, we cannot exclude aggregation phenomena of a different nature than those of π–π stacking interactions.

Electrochemical characterization

The electronic properties of Zn^{II} porphyrinates **1–3** have been investigated by cyclic voltammetry (CV) and compared to those of **4** previously determined,[27] working under the same experimental conditions (see ESI†). CV patterns obtained at 0.2 V s^{-1} on a glassy carbon electrode in DMF + 0.1 M TBAP (tetrabutylammonium perchlorate) are reported in Fig. S4,† and their key features are summarized in Table 2.

In all cases the first oxidation and reduction peaks are reversible or quasi-reversible from both the electrochemical and chemical point of view, affording the determination of formal potentials ($E^{\circ\prime}$ approximate standard potentials E° under the assumption of neglecting activity coefficients). From the $E^{\circ\prime}$ values the electrochemical HOMO and LUMO energy levels, and thus the HOMO–LUMO energy gap (E_g) were evaluated (Table 2),[34] employing ferrocenium/ferrocene redox couple as a reference for the intersolvental comparison of electrode potentials.[35,36]

Zn^{II} porphyrinates **1–3** have an electrochemical LUMO level at higher energy than that of the TiO_2 conduction band and an electrochemical HOMO level at a lower energy than that of the I^-/I_3^- redox couple, such that they may act as dyes in DSSCs (Fig. 3).

Dyes **2** and **3**, with the octyloxy chains at o,p- and o-positions, respectively, with respect to **4**, show LUMO levels at a higher
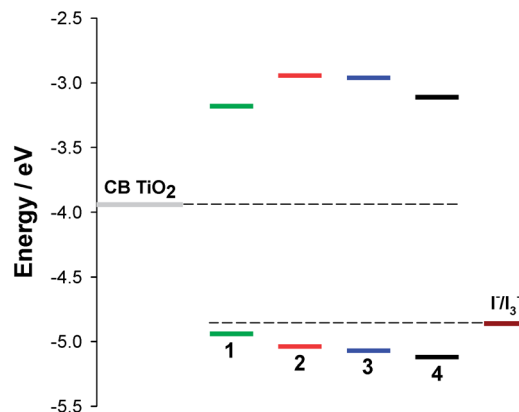
Fig. 3 HOMO–LUMO levels for **1**, **2**, **3** and **4**.

energy (−2.95 eV for **2** and −2.97 eV for **3** vs. −3.11 eV for **4**) and HOMO levels of slightly higher energy (−5.05 eV for **2** and −5.08 eV for **3** vs. −5.13 eV for **4**). The E_g for **2** and **3** is larger than that of **4** (2.10 eV and 2.11 eV for **2** and **3**, vs. 2.02 eV for **4**), a trend similar to that observed between dyes LD13 and LD14.[11]

On the contrary dye **1**, with the octyloxy chains at the o,o-positions, shows a LUMO level at slightly lower energy (−3.18 eV) and a HOMO level at higher energy (−4.94 eV), such that the E_g of **1** is surprisingly narrower by 0.25 eV compared to that of **4**.

The value of 1.77 eV for **1** is more similar to values measured for *meso* push–pull Zn^{II} porphyrinates (1.70–1.93 eV)[27,34] than those reported for β-mono- or disubstituted push–pull Zn^{II} tetraarylporphyrinates (1.95–2.12 eV)[27] under the same experimental conditions. It is known that the porphyrin ring shows an ambivalent donor or acceptor character, depending on the pull or push nature of the substituent;[32] however, according to our experimental experience, such a low value of the electrochemical HOMO–LUMO E_g has never been reported for this type of β-substituted dye. Such an interesting result suggests that the o,o-substitution of the four phenyl rings in this type of porphyrinc architecture may provide a relevant effect on the electronic structure, and therefore probably on the charge-transfer processes as also suggested by the low molar absorption coefficient of **1** when compared to **2–4** (Table 1).

Photoelectrochemical studies

The compounds referred to in this work were adopted as suitable light harvesting sensitizers in DSSCs, prepared using a

Table 2 Key CV features of dyes **1–4** and electrochemical energy levels HOMO and LUMO derived therefrom. $E_{Ic}^{\circ\prime}$ and $E_{Ia}^{\circ\prime}$ both refer to the ferrocene redox couple[35,36]

Dye	$E_{Ic}^{\circ\prime}$ (V/Fc$^+$|Fc)	LUMO (eV)	$\Delta E^{\circ\prime}$ (V) ($E_{g,\ EC}$/eV)	HOMO (eV)	$E_{Ia}^{\circ\prime}$ (V/Fc$^+$|Fc)
1	−1.62	−3.18	1.77	−4.94	0.14
2	−1.85	−2.95	2.10	−5.05	0.25
3	−1.83	−2.97	2.11	−5.08	0.28
4	−1.69	−3.11	2.02	−5.13	0.33

TiO$_2$ 15 μm double active layer with a 0.16 cm^2 area on FTO as the photoanode (see ESI†).

To obtain the best power conversion efficiencies, the TiO$_2$ layer on FTO was immersed for 4 h in an EtOH/THF 9 : 1 solution of each dye (0.2 mM) and the electrolyte Z960 (1.0 M 1,3-dimethylimidazolium iodide, 0.03 M I$_2$, 0.05 M LiI, 0.10 M guanidinium thiocyanate, and 0.50 M 4-*tert*-butylpyridine in acetonitrile/valeronitrile, 85 : 15)[37] was identified among different electrolytes tested by varying the components of the solution. The photovoltaic efficiencies of the DSSCs were also optimized by adding various amounts of chenodeoxycholic acid (CDCA) as a disaggregating agent. The addition of 2 mM of CDCA obtained the best results.

The *J–V* characteristics (see Fig. 4) and electrochemical impedance spectroscopy (EIS) analysis were investigated in the four dyes to assess performance.

Photovoltaic characteristics of these devices (measured under 1 sun illumination through an AM 1.5G filter) are summarized in Table 3. Details on device fabrication are reported in the ESI† section.

The power conversion efficiencies of DSSCs based on dyes **1–3** are 5.2%, 4.7% and 6.1%, respectively, showing a meaningful increment compared to reference dye **4**, which does not exceed 3.4% under the same test conditions (see Table 3).

In particular for **3**, we observed an increase of almost 80% in performance compared to **4**, therefore, showing a considerably higher increase in efficiency compared to that reported (9%) for *meso* push–pull Zn^{II} diarylporphyrinates.[11]

This enhancement is mainly attributed to the large increase of J_{SC}, from 7.1 mA × cm^{-2} for dye **4** to 11.8 mA × cm^{-2} for dye **3**. V_{OC} also increased from 630 mV for **4** to 694 mV for **3**, this latter value being particularly high if compared to V_{OC} values reported for other β-substituted Zn^{II} tetraarylporphyrinates used as dyes.[9,23,25,27]

The dye loading capabilities of the sensitizers (see Table 3) were estimated by UV-vis spectroscopy after desorption in alkaline solution. The lower surface concentration of **1** and **4** dyes (0.6 × 10^{-7} mol cm^{-2} and 0.4 × 10^{-7} mol cm^{-2}, respectively) with respect to that of dye **3** (1.2 × 10^{-7} mol cm^{-2}) can be

ascribed to the high steric hindrance of the substituents at the *ortho*-positions and *meta*-positions of the phenyl rings. On the other hand, it seems that the presence of a single long alkoxy chain in the *ortho*-position allows dye **3** to pack more favourably at the TiO$_2$ surface producing a better coverage of the semiconductor.

Incident monochromatic photon-to-current conversion efficiency (IPCE) spectra are presented in Fig. 5.

3 exhibits the highest IPCE yield, with a marked contribution from the Q-band region

In particular, the IPCE values in the Q-band region are relatively higher than the expected values from electronic absorption spectra for all dyes. This characteristic can be ascribed to the peculiar charge-transfer character of the Q-bands (essentially the HOMO–LUMO transition), as previously clarified by theoretical calculation.[27]

A careful EIS analysis has been carried out to investigate the charge-transfer processes at the interface TiO$_2$-dye/electrolyte. Charge transfer resistance (R_{ct}) and the chemical capacitance (C_μ) have been, thus, extrapolated from fitting the experimental data with an equivalent electrical model[38] (details are reported in ESI†). Because all devices were fabricated and tested under the same conditions, only the differences in the molecular structure of the sensitizers influenced the electrochemical parameters. Both R_{ct} and C_{means} have been plotted as a function of the corrected potential (see Fig. S4–S5†). From the analysis of C_μ plots, it may be deduced that there is no significant shift in the position of the conduction band edge for the three different
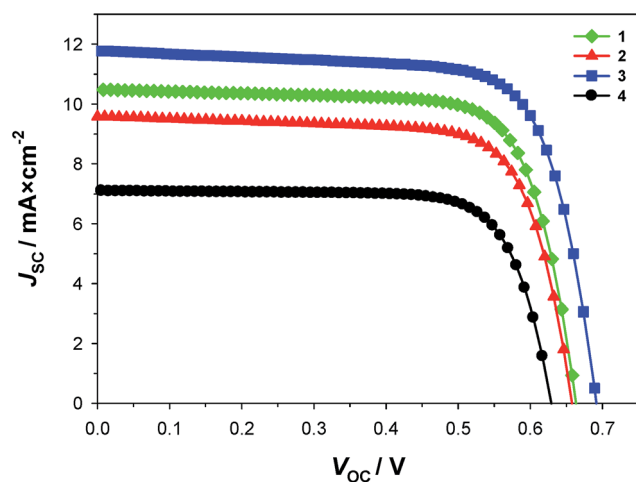
Table 3 Photovoltaic characteristics of DSSCs incorporating dyes **1–4**
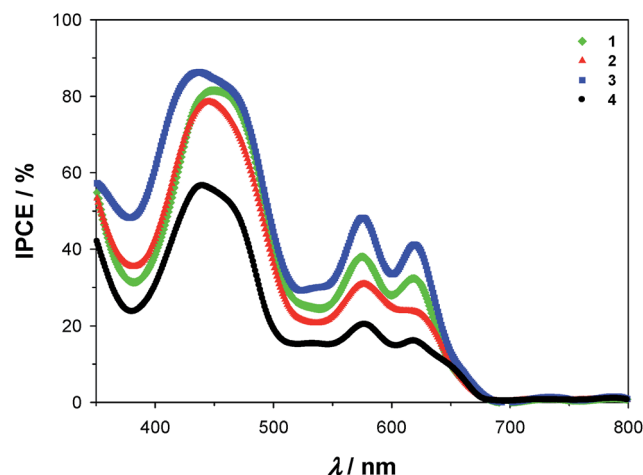
Dye	J_{SC}/mA cm^{-2}	V_{OC}/mV	FF	PCE/%	Dye loading/10^{-7} mol cm^{-2}
1	10.5	665	0.75	5.2	0.6
2	9.6	660	0.75	4.7	0.8
3	11.8	694	0.74	6.1	1.2
4	7.1	630	0.77	3.4	0.4

Fig. 4 Current–voltage characteristics of dyes **1–4**.

Fig. 5 IPCE spectra of DSSCs implementing dyes **1–4**.

This journal is © The Royal Society of Chemistry 2015

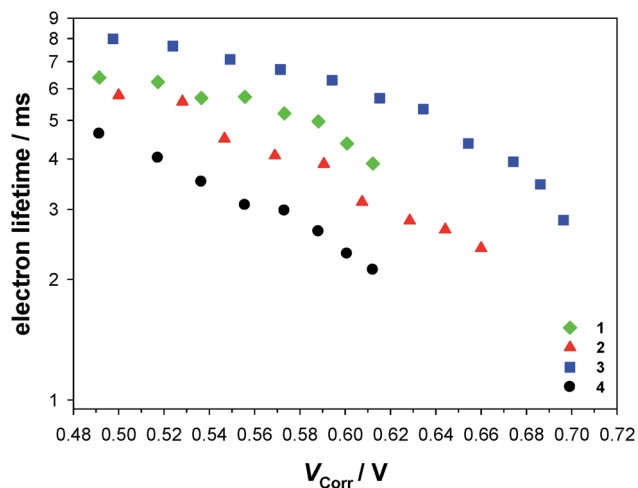*J. Mater. Chem. A*, 2015, **3**, 2954–2959 | **2957**

Fig. 6 Apparent electron lifetime as a function of the corrected potential for dyes **1–3** under illumination.

compounds: a shift of just 20 meV has been detected between dye **1** and dye **3**.

The trend observed for the R_{ct} plot (shown in Fig. S5†) is in agreement with the trend of V_{OC} values reported in Table 3: once again dye **3** exhibits the best condition to minimize the recombination of the photogenerated carriers, thus, justifying its highest open circuit potential with respect to dyes **1** and **2**.

Hence, the same trend was revealed for the electron lifetime (as shown in Fig. 6), calculated by the equation: $\tau = R_{ct} \times C_\mu$ using different values.

These differences recall the effect of recombination phenomena associated to intermolecular quenching or detrimental charge transfer between photoinjected electrons and the triiodide acceptor. The presence of relatively extended alkyloxy chains could have two opposite effects: on the one hand, they may reduce π–π aggregation, but on the other hand, by enveloping the porphyrinic rings, they can turn them into hydrophobic spheres, which have difficulty in interacting with the hydrophilic TiO$_2$ surface. In fact, a large amount of CDCA (10 times more concentrated than dyes **1–3**) was necessary to make the TiO$_2$ surface a more lipophilic environment, in order to support dye loading. In addition, CDCA also represents a competitor agent in the coverage of the TiO$_2$ surface.

Therefore, it is reasonable to suppose that in the case of dye **1** the two long chain substituents create an 'organic barrier', which reduces detrimental recombination effects and provides a relatively high photovoltage, despite the lower position of its LUMO level in comparison to dyes **2–4**. On the other hand, it appears that for dye **3** these competing properties are well balanced, giving the higher photoconversion efficiency.

Conclusions

We report for the first time the synthesis of three new β-substituted Zn^{II} tetraarylporphyrinate dyes (**1–3**) for DSSCs, bearing octyloxy chains at the o,o-, o,p- or o-positions of the four phenyl groups, respectively, and their electronic absorption

spectra and electrochemical features, which are strongly influenced by the alkoxy group position.

We have successfully applied an In^{III}-salt catalyst for the synthesis of a o,o-alkoxy tetraarylporphyrin in just one step instead of almost three steps as previously reported.[29] Surprisingly, compound **1** (–OC$_8$H$_{17}$ in o,o-positions) has shown particular spectroscopic and electrochemical characteristics, if compared to those of the isomer compound **2** (–OC$_8$H$_{17}$ in o,p-positions). In particular **1** has a narrower electrochemical HOMO–LUMO energy gap (1.77 eV $vs.$ 2.10 eV for **2**) that is more similar to those of $meso$ push–pull Zn^{II} tetraarylporphyrinates, with a higher charge-transfer character,[18] recorded in the same experimental conditions.[34]

If we consider that **1** is easier to oxidize, this could be explained by inductive and/or mesomeric effects (similar for o- and p-substituents), but also by its peculiar structure, where four oxygen atoms are above the porphyrin ring plain and the other four oxygen atoms are below it: the electronic cloud above and below the porphyrin is therefore richer in electrons, thus reducing the first oxidation potential (0.14 V for **1** $vs.$ 0.25 V for **2**).

With **1–3** acting as dyes in DSSCs, we found that the introduction of alkoxy chains significantly improves photovoltaic performance, compared to that of **4**, considered as a reference dye and already characterized by the presence of sterically bulky t-butyl groups. Moreover, this effect on β-substituted Zn^{II} tetraarylporphyrinate dyes is much higher than that reported for $meso$ push–pull Zn^{II} diarylporphyrinates.[11]

Our experimental results indicate that the best dye of the series is the simpler dye **3**, with only one octyloxy chain in o-position of each phenyl ring, showing an almost 80% increase in power conversion efficiency if compared to that of reference dye **4** under the same test conditions.

Even if this interesting result is related to a very high V_{OC} for a tetraarylporphyirinic dye and a good FF, dye **3** nonetheless exhibits a rather low J_{SC} value if compared to the best results reported for porphyrin-sensitized solar cells. Such J_{SC} value probably depends on the high concentration of CDCA used. In fact, alkoxy chains in o-position can prevent the aggregation phenomena of π–π nature, but may produce a lipophilic sphere around the porphyrinic core, which makes dye loading difficult. For this reason we intend to investigate alkoxy chains of different lengths and nature in order to find the right balance to prevent the aggregation and to improve dye loading.

Acknowledgements

Notes and references

1 A. Hagfeldt, G. Boschloo, L. Sun, L. Kloo and H. Pettersson, *Chem. Rev.*, 2010, **110**, 6595–6663.

2 M. K. Nazeeruddin, A. Kay, I. Rodicio, R. Humphry-Baker, E. Müller, P. Liska, N. Vlachopoulos and M. Grätzel, *J. Am. Chem. Soc.*, 1993, **115**, 6382–6390.

3 M. K. Nazeeruddin, F. De Angelis, S. Fantacci, A. Selloni, G. Viscardi, P. Liska, S. Ito, B. Takeru and M. Grätzel, *J. Am. Chem. Soc.*, 2005, **127**, 16835–16847.

4 Q. Yu, Y. Wang, Z. Yi, N. Zu, J. Zhang, M. Zhang and P. Wang, *ACS Nano*, 2010, **4**, 6032–6038.

5 L. L. Li and E. W. G. Diau, *Chem. Soc. Rev.*, 2013, **42**, 291–304.

6 T. Bessho, S. M. Zakeeruddin, C. Y. Yeh, E. W. G. Diau and M. Grätzel, *Angew. Chem., Int. Ed.*, 2010, **49**, 6646–6649.

7 K. Hara, in *Molecular Catalysts for Energy Conversion*, ed. T. Okada and M. Kaneko, Springer-Verlag Berlin, Berlin, 2009, pp. 217–250.

8 A. J. Mozer, P. Wagner, D. L. Officer, G. G. Wallace, W. M. Campbell, M. Miyashita, K. Sunahara and S. Mori, *Chem. Commun.*, 2008, 4741–4743.

9 M. J. Griffith, K. Sunahara, P. Wagner, K. Wagner, G. G. Wallace, D. L. Officer, A. Furube, R. Katoh, S. Mori and A. J. Mozer, *Chem. Commun.*, 2012, **48**, 4145–4162.

10 C.-L. Wang, C.-M. Lan, S.-H. Hong, Y.-F. Wang, T.-Y. Pan, C.-W. Chang, H.-H. Kuo, M.-Y. Kuo, E. W.-G. Diau and C.-Y. Lin, *Energy Environ. Sci.*, 2012, **5**, 6933–6940.

11 Y. C. Chang, C. L. Wang, T. Y. Pan, S. H. Hong, C. M. Lan, H. H. Kuo, C. F. Lo, H. Y. Hsu, C. Y. Lin and E. W. G. Diau, *Chem. Commun.*, 2011, **47**, 8910–8912.

12 C. Y. Lee and J. T. Hupp, *Langmuir*, 2010, **26**, 3760–3765.

13 C. Y. Lee, C. She, N. C. Jeong and J. T. Hupp, *Chem. Commun.*, 2010, **46**, 6090–6092.

14 A. Yella, H. W. Lee, H. N. Tsao, C. Yi, A. K. Chandiran, M. K. Nazeeruddin, E. W. G. Diau, C. Y. Yeh, S. M. Zakeeruddin and M. Grätzel, *Science*, 2011, **334**, 629–634.

15 C. Yi, F. Giordano, N. L. Cevey-Ha, H. N. Tsao, S. M. Zakeeruddin and M. Grätzel, *ChemSusChem*, 2014, **7**, 1107–1113.

16 A. Yella, C. L. Mai, S. M. Zakeeruddin, S. N. Chang, C. H. Hsieh, C. Y. Yeh and M. Grätzel, *Angew. Chem., Int. Ed.*, 2014, **53**, 2973–2977.

17 S. Mathew, A. Yella, P. Gao, R. Humphry-Baker, F. E. CurchodBasile, N. Ashari-Astani, I. Tavernelli, U. Rothlisberger, K. NazeeruddinMd and M. Grätzel, *Nat. Chem.*, 2014, **6**, 242–247.

18 A. Orbelli Biroli, F. Tessore, M. Pizzotti, C. Biaggi, R. Ugo, S. Caramori, A. Aliprandi, C. A. Bignozzi, F. De Angelis,

19 G. Giorgi, E. Licandro and E. Longhi, *J. Phys. Chem. C*, 2011, **115**, 23170–23182.

19 B. J. Littler, M. A. Miller, C.-H. Hung, R. W. Wagner, D. F. O'Shea, P. D. Boyle and J. S. Lindsey, *J. Org. Chem.*, 1999, **64**, 1391–1396.

20 J. K. Laha, S. Dhanalekshmi, M. Taniguchi, A. Ambroise and J. S. Lindsey, *Org. Process Res. Dev.*, 2003, **7**, 799–812.

21 J. S. Lindsey, *Acc. Chem. Res.*, 2009, **43**, 300–311.

22 M. O. Senge, *Chem. Commun.*, 2011, **47**, 1943–1960.

23 W. M. Campbell, A. K. Burrell, D. L. Officer and K. W. Jolley, *Coord. Chem. Rev.*, 2004, **248**, 1363–1379.

24 A. W. I. Stephenson, P. Wagner, A. C. Partridge, K. W. Jolley, V. V. Filichev and D. L. Officer, *Tetrahedron Lett.*, 2008, **49**, 5632–5635.

25 W. M. Campbell, K. W. Jolley, P. Wagner, K. Wagner, P. J. Walsh, K. C. Gordon, L. Schmidt-Mende, M. K. Nazeeruddin, Q. Wang, M. Grätzel and D. L. Officer, *J. Phys. Chem. C*, 2007, **111**, 11760–11762.

26 M. Erdélyi and A. Gogoll, *J. Org. Chem.*, 2001, **66**, 4165–4169.

27 G. Di Carlo, A. Orbelli Biroli, M. Pizzotti, F. Tessore, V. Trifiletti, R. Ruffo, A. Abbotto, A. Amat, F. De Angelis and P. R. Mussini, *Chem.–Eur. J.*, 2013, **19**, 10723–10740.

28 K. Ohta, H. D. Nguyen-Tran, L. Tauchi, Y. Kanai, T. Megumi and Y. Takagi, *Handbook of Porphyrin Science with Applications to Chemistry, Physics, Materials Science, Engineering, Biology and Medicine Applications*, 2011, vol. 12, pp. 1–120.

29 C. Arunkumar, P. Bhyrappa and B. Varghese, *Tetrahedron Lett.*, 2006, **47**, 8033–8037.

30 E. Tsuchida, T. Komatsu, E. Hasegawa and H. Nishide, *J. Chem. Soc., Dalton Trans.*, 1990, 2713–2718.

31 B. M. Smith, S. D. Kean, M. F. Wyatt and A. E. Graham, *Synlett*, 2008, 1953–1956.

32 E. Annoni, M. Pizzotti, R. Ugo, S. Quici, T. Morotti, M. Bruschi and P. Mussini, *Eur. J. Inorg. Chem.*, 2005, **2005**, 3857–3874.

33 J. C. Earles, K. C. Gordon, A. W. I. Stephenson, A. C. Partridge and D. L. Officer, *Phys. Chem. Chem. Phys.*, 2011, **13**, 1597–1605.

34 P. R. Mussini, A. Orbelli Biroli, F. Tessore, M. Pizzotti, C. Biaggi, G. Di Carlo, M. G. Lobello and F. De Angelis, *Electrochim. Acta*, 2012, **85**, 509–523.

35 G. Gritzner and J. Kuta, *Pure Appl. Chem.*, 1984, **56**, 461–466.

36 G. Gritzner, *Pure Appl. Chem.*, 1990, **62**, 1839–1858.

37 E. M. Barea, V. Gónzalez-Pedro, T. Ripollés-Sanchis, H. P. Wu, L. L. Li, C. Y. Yeh, E. W. G. Diau and J. Bisquert, *J. Phys. Chem. C*, 2011, **115**, 10898–10902.

38 J. Bisquert, F. Fabregat-Santiago, I. Mora-Seró, G. Garcia-Belmonte and S. Giménez, *J. Phys. Chem. C*, 2009, **113**, 17278–17290.

This journal is © The Royal Society of Chemistry 2015

J. Mater. Chem. A, 2015, **3**, 2954–2959 | **2959**